Scanning Electron Microscopy Studies of Polymer Melt Devolatilization

The devolatilization mechanism of polystyrene was studied by scanning electron microscopy. Strands of molten polystyrene, containing 2,300 ppm styrene, and molten polystyrene containing 5% pentane, were extruded into a heated vacuum chamber. The strands were abruptly frozen, then fractured under liquid nitrogen and their morphology studied with scanning electron microscopy. A rich variety of morphological features in the core and on the surface of strands was discovered. These include micro- and miniblisters, fibrous structures, and crusty nodules on the inner surfaces of large macrobubbles. The source of these morphological features and their relevance to devolatilization is discussed.

R. J. Albalak, Z. Tadmor and Y. Talmon
Department of Chemical Engineering
Technion-Israel Institute of Technology
Haifa 32000, Israel

Introduction

Residual unreacted monomer, solvent, diluents, and low molecular weight reaction products are frequently removed from molten polymer in a devolatilization step. Industrially, the process is carried out either in so-called falling-strand devolatilizers or in rotating devolatilizers (Biesenberger and Sebastian, 1983; Denson, 1985). The former are adaptations of ordinary flash tanks to high-viscosity molten polymers; the latter type are adaptations of classical polymer processing machinery such as single- and twin-screw extruders and thin-film evaporators to polymer melt devolatilization. In rotating-type equipment the characteristic mechanistic feature of the process is a rolling pool of melt out of which a thin film is continuously deposited onto a moving surface and recollected into the pool (Biesenberger and Sebastian, 1983). Figure 1 shows schematically the falling-strand and the rolling-pool/thin-film devolatilization processes. In either case the hot polymeric solution is suddenly supersaturated by exposing it to high vacuum. The volatile component is removed from the solution by a complex bubble transport mechanism.

Newman and Simon (1980) were the first to analyze and discuss in detail the mechanism of devolatilization in falling-strand devolatilizers. They view the process as one of molecular diffusion into a swarm of bubbles, and expansion of those bubbles against surface tension and viscous forces. In their mathematical model they calculated the growth of a single bubble, and the corresponding solvent depletion in a unit volume of polymer solution. They used finite-difference integration of a system of simplified differential equations based on penetration theory, corrected for convective effects due to bubble expansion and the extended Rayleigh equation for bubble growth. Bubble nucleation was not considered because they assumed that the devolatilizer is fed with a melt stream that is already swollen with vapor bubbles from the previous processing step. Bubble coalescence and rupture was assumed to occur suddenly and uniformly throughout the foamed-up solution. Their model compared favorably with experimental data on a polystyrene-styrene devolatilizer in a temperature range of 200 to 250°C and with an initial concentration of styrene from 1,500 to 12,500 ppm.

The present study was undertaken to elucidate on a microscopic scale the details of the devolatilization process by extruding strands of molten polymeric solutions into a vacuum chamber and suddenly freezing them. The objective of the study was to experimentally measure the concentration and size distribution of bubbles as a function of time, and to obtain direct experimental verification of theoretical models such as the Newman-Simon model, or appropriate improvements thereof. Contrary to expectations, the detailed scanning electron microscopy study of the frozen strands revealed instead of swarms of bubbles in various stages of growth, a surprisingly rich variety of new morphological features, which seems to indicate that the devolatilization mechanism in falling-strand devolatilizers, and perhaps all devolatilizers, is far more complex than generally assumed and expected.

Experimental Method

The experimental system consists of a melt flow indexer (MFI) that produces the polymer melt, and an evacuated brass

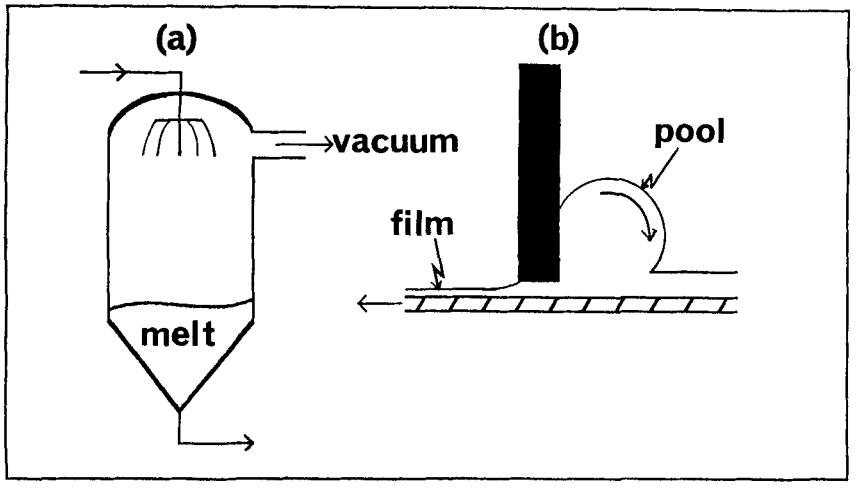

Figure 1. a. Strand-type devolatilizer
b. Rolling-pool/thin-film mechanism

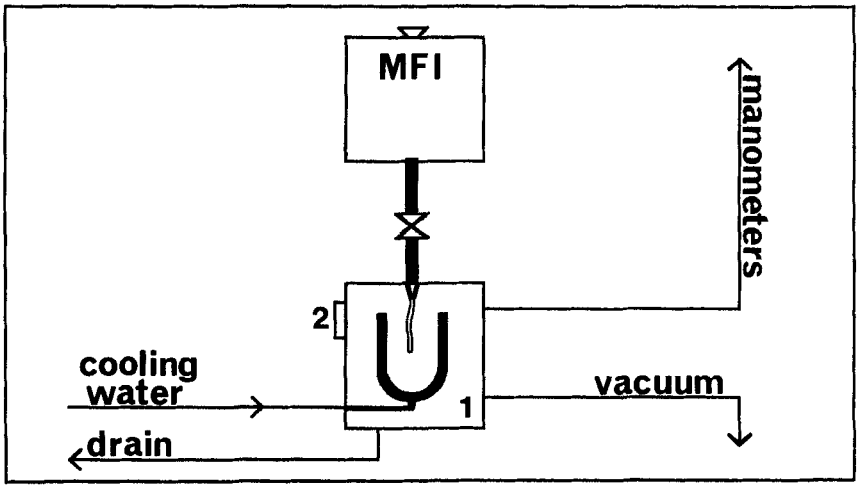

Figure 2. Experimental setup.
MFI, melt flow index apparatus
1. Temperature-controlled brass chamber with U-shaped spraying device
2. Glass viewing port

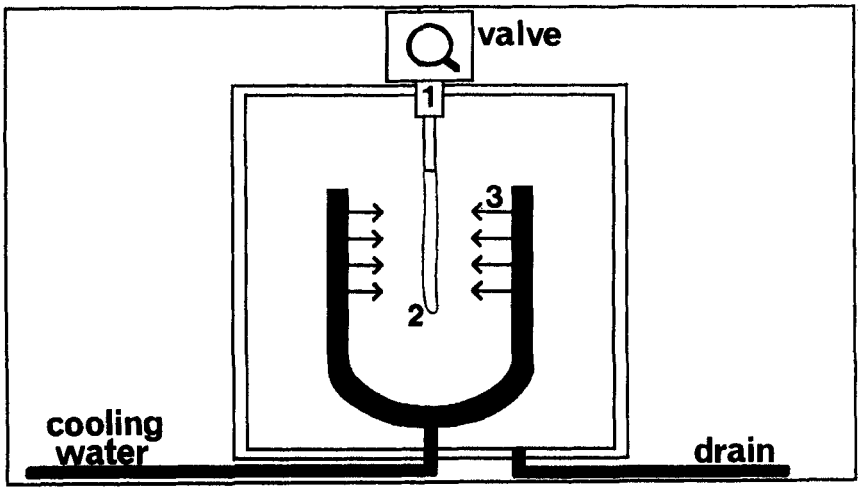

Figure 3. Details of brass chamber.
1. Die; 2. polymer strand; 3. water jets

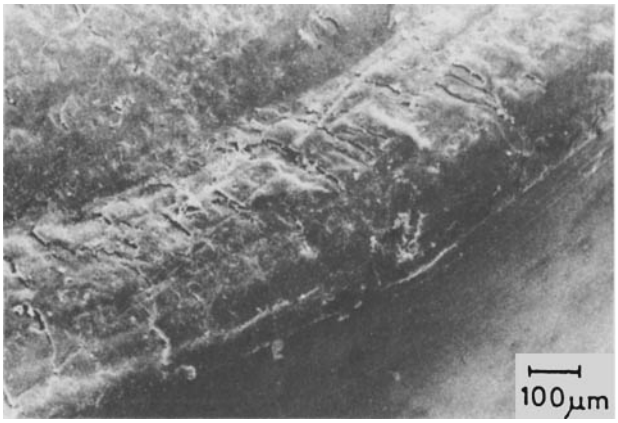

Figure 4. PS-styrene sample extruded at 180°C into atmospheric pressure.
The micrograph shows the smooth lateral surface and part of the crossection; there is no evidence of bubbles.

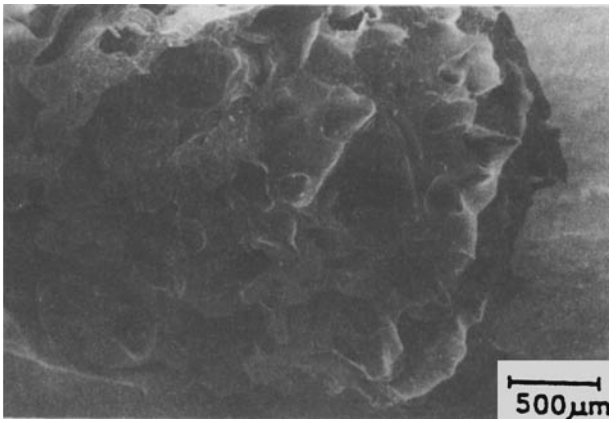

Figure 6. Preextruded PS sample pressed through MFI die at 180°C into 1.3 kPa pressure.
PS beads were shaped into a rodlike product, and a rod that appeared to be clean from entrained air was loaded into the MFI. The micrograph shows the characteristic macrobubble morphology.

chamber into which a thin strand of melt is extruded through a die, as indicated in Figure 2. A valve connects the MFI to the bottom chamber. The whole system is electrically heated by three heating elements controlled in the range of 170 to 235°C by three independent on-off controllers. The bottom chamber is connected to a rotary vacuum pump. The pressure, in the range of 90 Pa (0.7 mm Hg) to atmospheric pressure, is measured by a set of manometers. Polymer pellets are fed into the MFI through its funnel-shaped top, and are compressed by a plunger loaded with weights. The molten polymer strand is frozen in the bottom chamber at any desired moment by cooling water sprayed on it through a U-shaped spraying device, Figure 3.

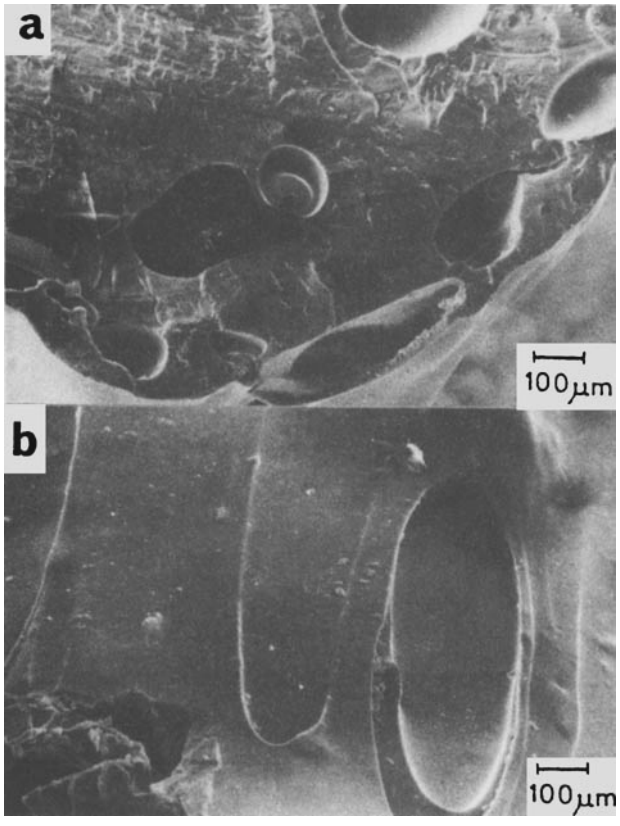

Figure 5. PS-styrene samples extruded into 100 Pa pressure.
a. Cross section (170°C)
b. Lateral surface (180°C)
Large macrobubbles are evident over both surfaces.

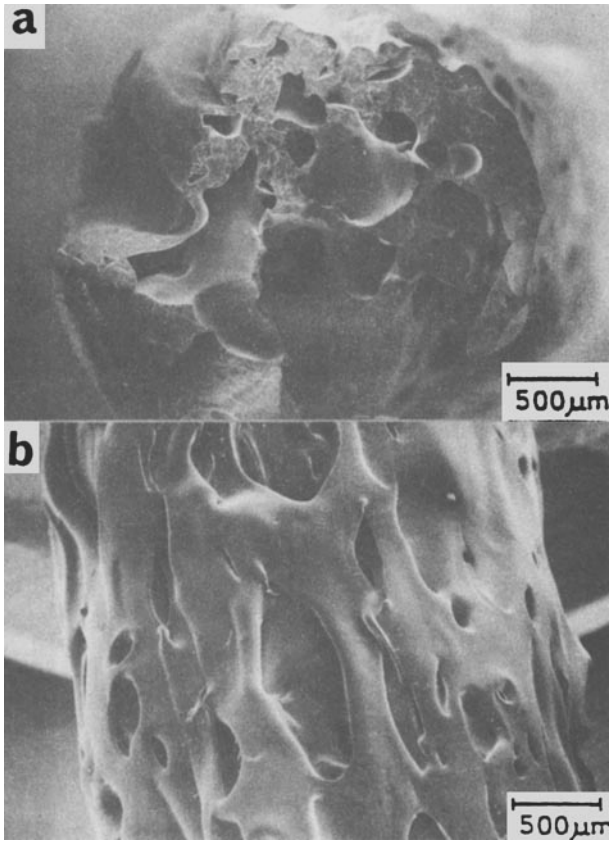

Figure 7. PS-styrene samples containing a small amount of fine dust extruded at 180°C into 100 Pa pressure.
a. Cross section
b. Lateral surface
Both surfaces are profusely covered with macrobubbles.

After freezing, scanning electron microscope (SEM) samples are prepared. The frozen strand, usually with a cross section of 2–4 mm, is detached from the die and is fractured in liquid nitrogen to expose its inner structure. In most experiments three such fractures were produced, revealing cross sections of different residence times in the vacuum chamber. The fractured pieces were trimmed to a height of about 7 mm and glued to cylindrical brass specimen holders (1 cm dia., 5 mm high) using Duco cement and colloidal silver cement. The specimens were then sputter-coated with a 25 nm gold layer. The colloidal silver cement and the gold coating prevent deleterious negative charge buildup in the specimen as it is scanned by the electron beam in the SEM.

The specimens were examined in a JEOL T-300 scanning electron microscope in the secondary electron imaging (SEI) mode, using an electron acceleration voltage of 25 kV. The fracture surface (cross section) and lateral area of each specimen were examined at different specimen tilt angles. A series of four to six micrographs of the same area were taken at magnifications of 35, 100, 350, 1,000, 3,500, and 10,000 times. These fixed magnification values facilitated comparison between different series of micrographs and allowed easy recognition of structural features as the magnification was increased.

The materials used in this study were a general-purpose polystyrene containing an initial concentration of approximately 2,300 ppm styrene, and a general-purpose polystyrene containing 5% pentane, prepared by pentane steeping of suspension beads. The initial and final volatile concentrations were determined by gas chromatography.

Results and Discussion

The molten polystyrene (PS) samples were extruded in a temperature range of 170 to 235°C into the heated vacuum chamber maintained at absolute pressures ranging from 100 Pa (0.8 mm Hg) to atmospheric pressure. The partial pressure of styrene vapor over a 2,300 ppm solution of polystyrene is of the order of 4 kPa (30 mm Hg) at 170°C and 12 kPa (90 mm Hg) at 235°C, therefore PS-styrene samples extruded into a much lower absolute pressure (i.e., of the order of 100 Pa) were substantially superheated. Such levels of superheat of course invite boiling phenomena. The superheat of the samples containing 5% pentane is much higher than of those containing styrene as the sole volatile component.

A micrograph of a polystyrene sample extruded at 180°C into atmospheric pressure is shown in Figure 4. This served as a reference sample. There is no superheat at this experimental condition, no boiling-foaming was expected to happen, and results indeed show no evidence of bubbles, either on the lateral surface or on the cross section.

Macrobubbles

The first characteristic morphological feature that appeared in samples extruded into high vacuum is a swarm of randomly

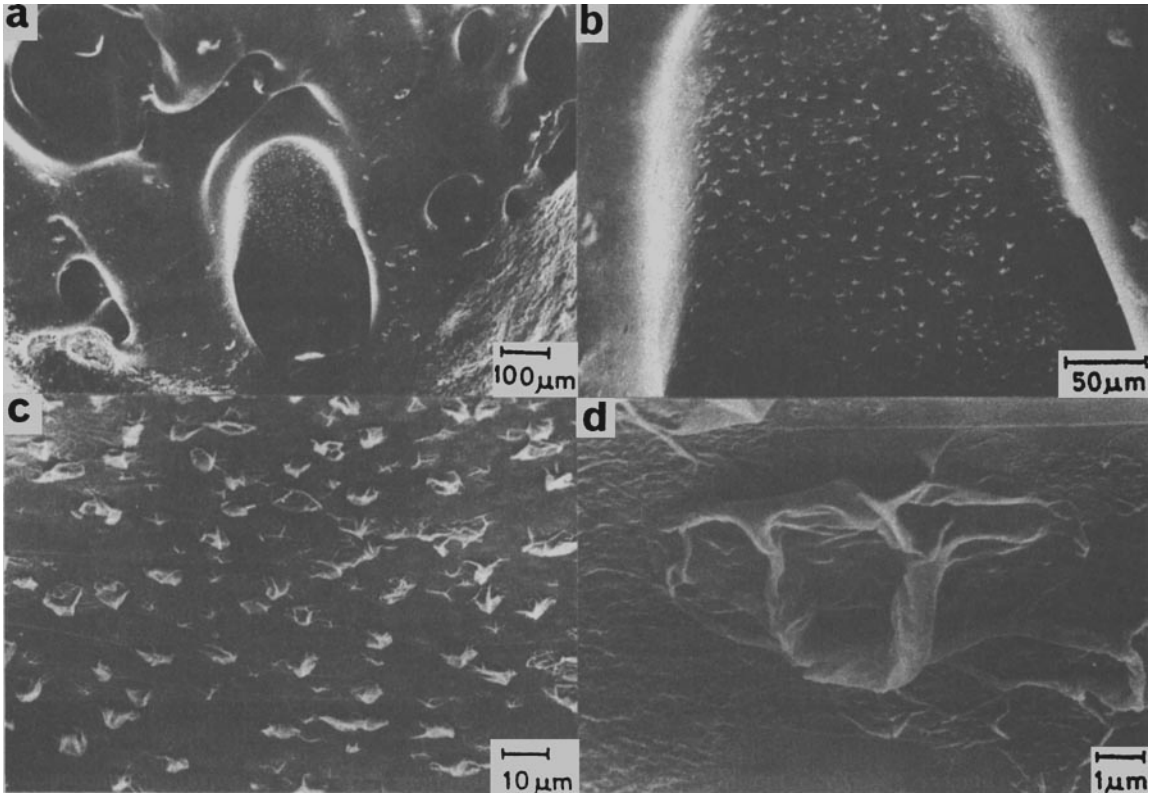

Figure 8. An area of lateral surface of a PS-styrene sample extruded at 200°C into 200 Pa pressure.

a. Lowest magnification shows macrobubbles and blister-covered inner surface
b. Inner surface of macrobubble at large magnification
c. Randomly scattered collapsed blisters
d. A single collapsed blister

scattered relatively large voids. These voids, termed "macrobubbles," of the order of 100 μm and above, are clearly seen on the cross section, Figure 5a, and on the lateral surface, Figure 5b, of samples extruded at 170°C and 180°C, respectively, into 100 Pa (1 mm Hg) pressure.

The exact origin and nature of the macrobubbles is still an open question. There are a number of possible explanations. First, macrobubbles may simply be the result of expanded free entrained noncondensable gas (e.g., air). Some air, for example, may be entrained between the beads of PS during the melting step in the barrel of the MFI. However, PS extruded at 200°C into 13 kPa pressure, that is, into absolute pressure above the partial vapor pressure of the styrene in the sample, showed practically no evidence of macrobubbles, although free entrained air at this vacuum level should have visibly expanded into bubbles. This finding seems to indicate that macrobubbles are not simply expanded free entrained air. This conclusion is further supported by an experiment carried out with a PS sample that was preextruded. In this experiment the PS beads were first extruded into a rodlike product on a laboratory single-screw extruder, and then charged into the MFI and extruded as usual into high vacuum. If macrobubbles originate from entrained free air, the screw extrusion step should have eliminated much of the entrained air, and no macrobubbles should be visible in the final micrographs. Yet in the micrograph shown in Figure 6, prepared from the preextruded sample pressed through the MFI at 180°C into 1.3 kPa pressure, macrobubbles appear profusely over the whole cross section. In fact, it appears that preextrusion even increased the number of macrobubbles. The reasons for this phenomenon are not clear. Finally, there is a further reason why it is unlikely that the macrobubbles are simply the result of the expansion of entrained free air. The inner surface of the macrobubbles is covered with morphological features that suggest a bubble growth process fed by volatile evaporation. Hence, the macrobubbles should also contain vapors of the volatiles and not only air. Perhaps they contain predominantly vapor and only traces of air.

This leads to a second alternative possible explanation asso-

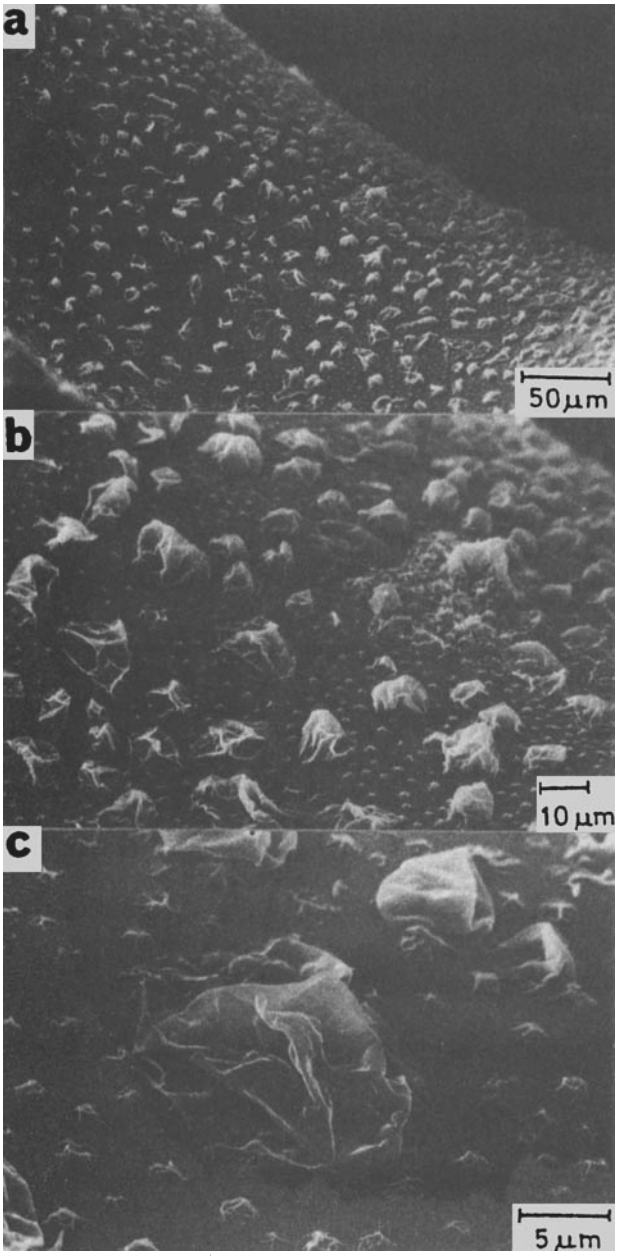

Figure 9. PS-styrene sample extruded at 235°C, into 300 Pa pressure.

Three magnifications showing miniblisters and microblisters on inner surface of a macrobubble within the core of the strand.

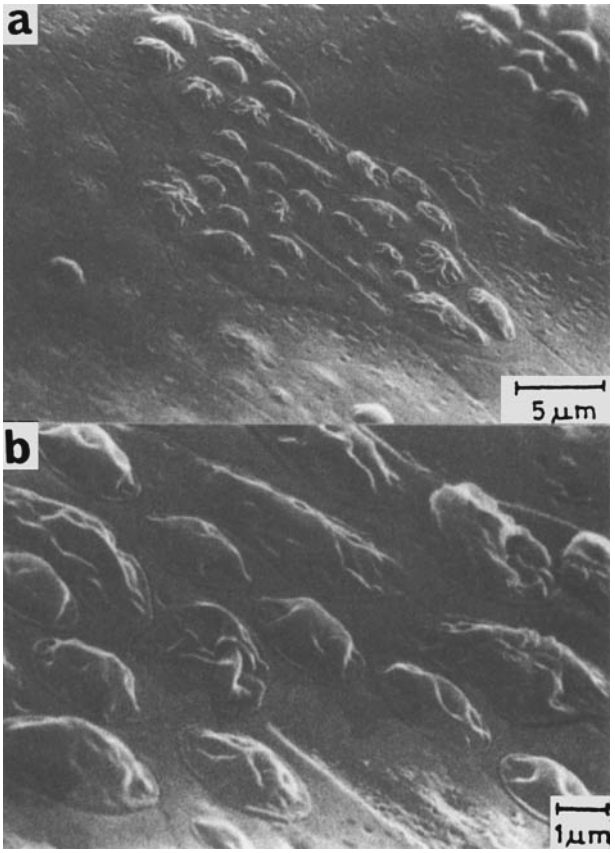

Figure 10. Lateral surface of a PS-styrene sample extruded at 170°C into 100 Pa pressure.

Two magnifications of the same area show microblisters growing on the remains of collapsed miniblisters.

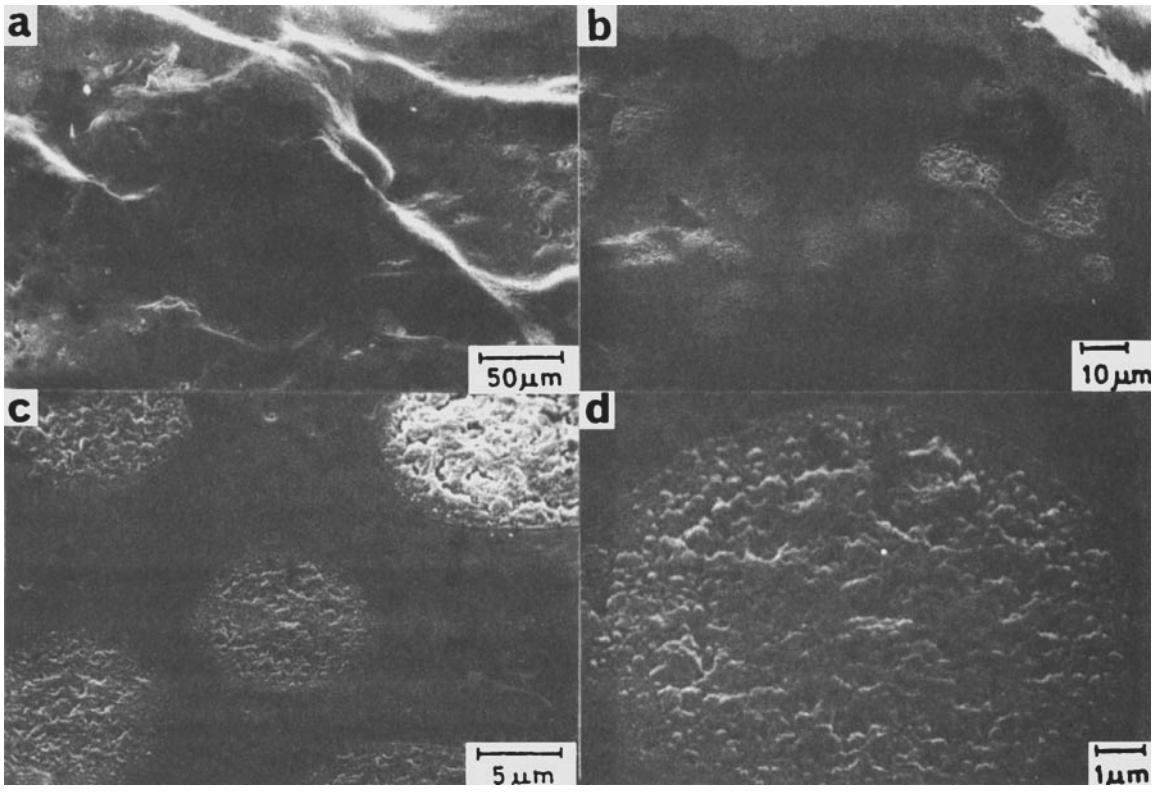

Figure 11. Strand cross section of a PS-styrene sample extruded at 170°C into 100 Pa pressure.
Coarse circular areas are the remains of miniblisters; small circular indentations are those of the microblisters.

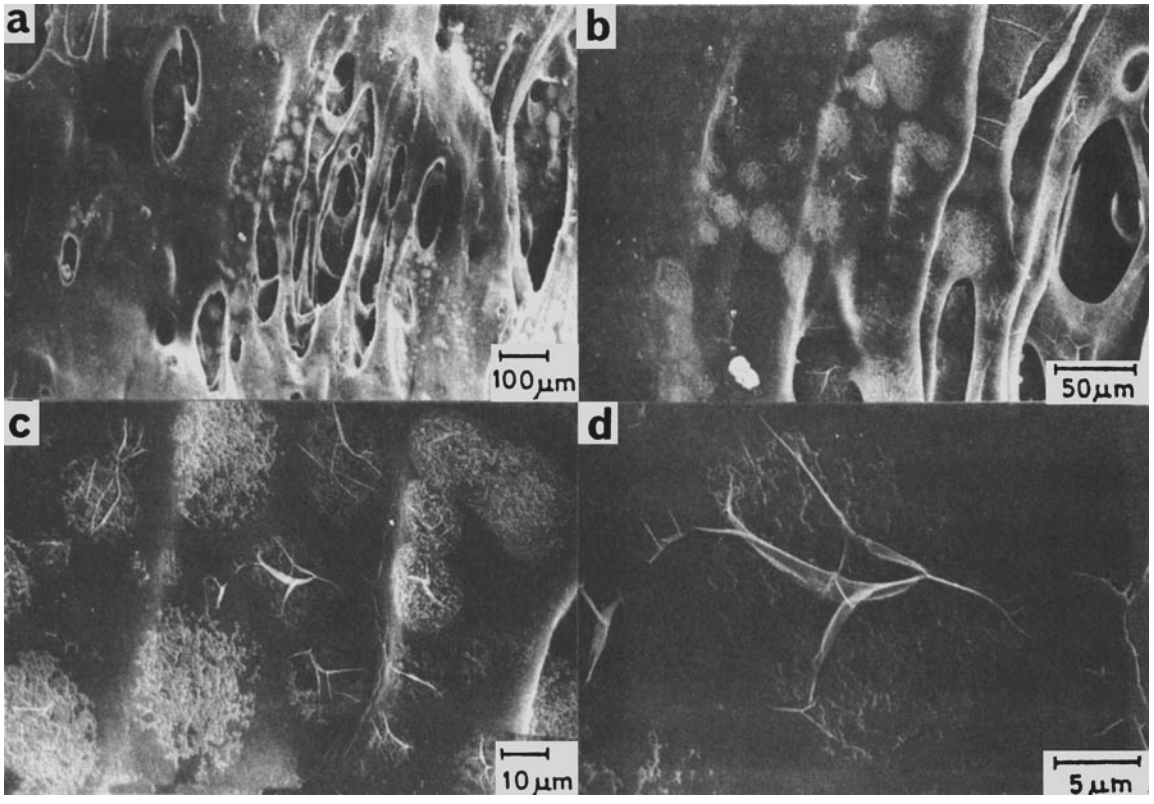

Figure 12. Lateral surface of a PS with 5% pentane sample extruded at 170°C into 100 Pa pressure.
The circular remains and collapsed skin of miniblisters are evident.

ciated with free air. Namely, that some free entrained air in the form of fine microbubbles is retained in the extruded strands, and these microbubbles serve as nuclei for bubble growth. They are then blown into macrobubbles by the evaporation of volatiles. Possibly the observation of an increase in macrobubble density observed with the preextruded PS sample, is due to an enhanced dispersion of free air into fine microbubbles in the course of the screw extrusion process, thus lending some indirect support to this "free air microbubble nuclei" hypothesis.

Yet another explanation of the origin of the microbubbles may be the presence of moisture in the system. Moisture may be absorbed in the PS or adsorbed onto the pellet surfaces. In the case of the pentane-containing PS, moisture may also be occluded in the beads. No special precautions were taken to dry the PS, although it was recognized that water frequently serves as a devolatilizing-foaming aid. However, it is unlikely that adsorbed moisture plays a dominant role in macrobubble formation, because in that case the PS sample extruded at 200°C into 13 kPa pressure, and even that extruded into atmospheric pressure, should have shown evidence of bubble formation. This was not the case. Moreover, adsorbed moisture should have led to a partially foamed extrudate with surface irregularities in the preextrusion step. Neither is it reasonable to assume that a minute amount of occluded moisture in the rich volatile pentane-containing PS samples, can play a dominant role in the macrobubble formation process of these samples. Finally, the homogeneously absorbed moisture may of course participate in the macrobubble formation process. This type of moisture, however, can be viewed as an additional volatile component of the styrene.

The last possible explanation proposed here excludes any role of free entrained noncondensable gas or of moisture in the macrobubble formation process. According to this explanation, the macrobubbles are the final stage of a growth process of vapor-filled bubbles in the natural course of boiling. The bubbles according to this explanation nucleate heterogeneously on stable Harvey-type nuclei (Harvey et al. 1944a,b) on entrained solid particles (e.g., dust particles). The mechanism is similar to the cavitation phenomena in ordinary liquids, which is also explained by heterogeneous nucleation in the bulk of the liquid on Harvey-type entrained nuclei (Hammit, 1980). However, if the macrobubbles grow out of entrained solid nuclei why are there relatively so few macrobubbles per unit volume? Is it because there are only a few active nuclei? Or perhaps once a nucleus starts growing the probability of activating additional neighboring nuclei diminishes? Figure 7 shows micrographs of a PS sample containing a small percentage of very fine dust. The experiment was done to show the possible effect of increased number of stable Harvey-type nuclei. The number of macrobubbles appears to have increased. But dust particles may also carry with them entrained free air as well as moisture, and we cannot safely attribute the increase in number of macrobubbles to increased number of nuclei. Thus, the question of the exact source of macrobubbles remains open.

It is worthwhile to note that in some commercial devolatilization operations there may be entrained noncondensable gas as

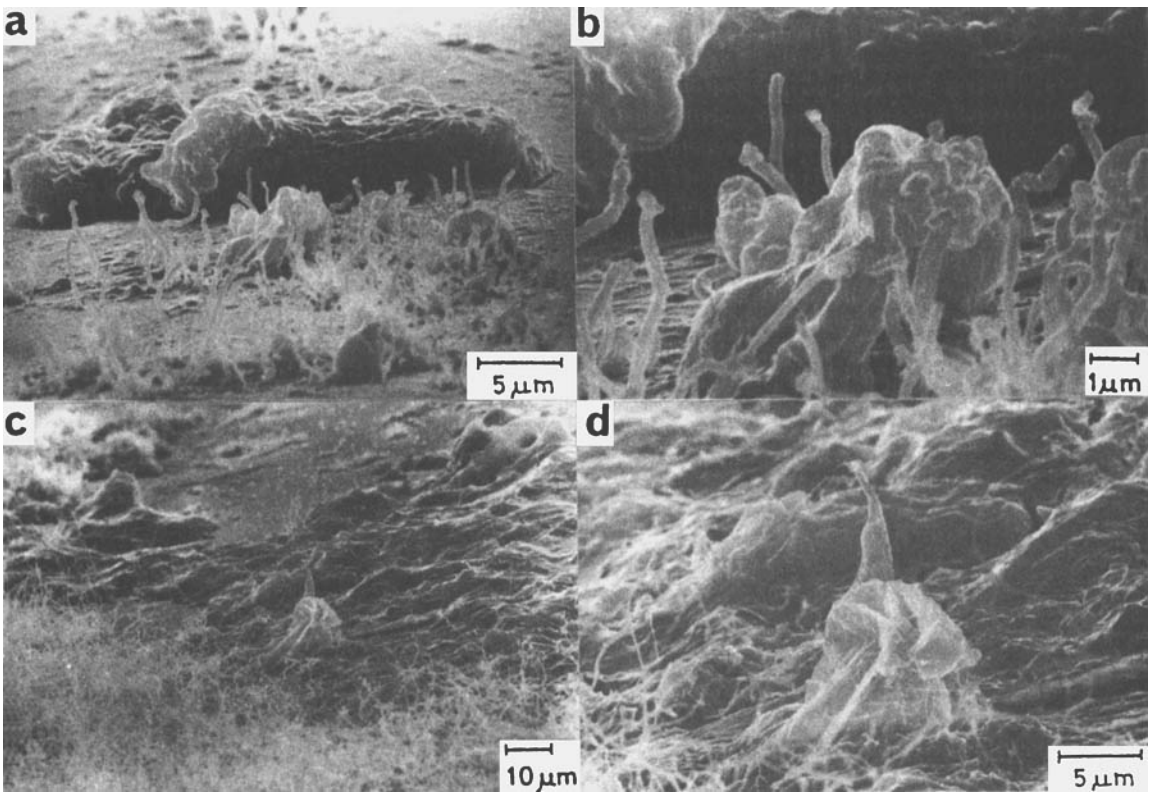

Figure 13. Stages in transformation of miniblisters into 'fibrous hairlike' structure; PS-styrene sample extruded at 200°C into 100 Pa pressure.

a, b. Lateral surface of strand
c, d. Two different areas

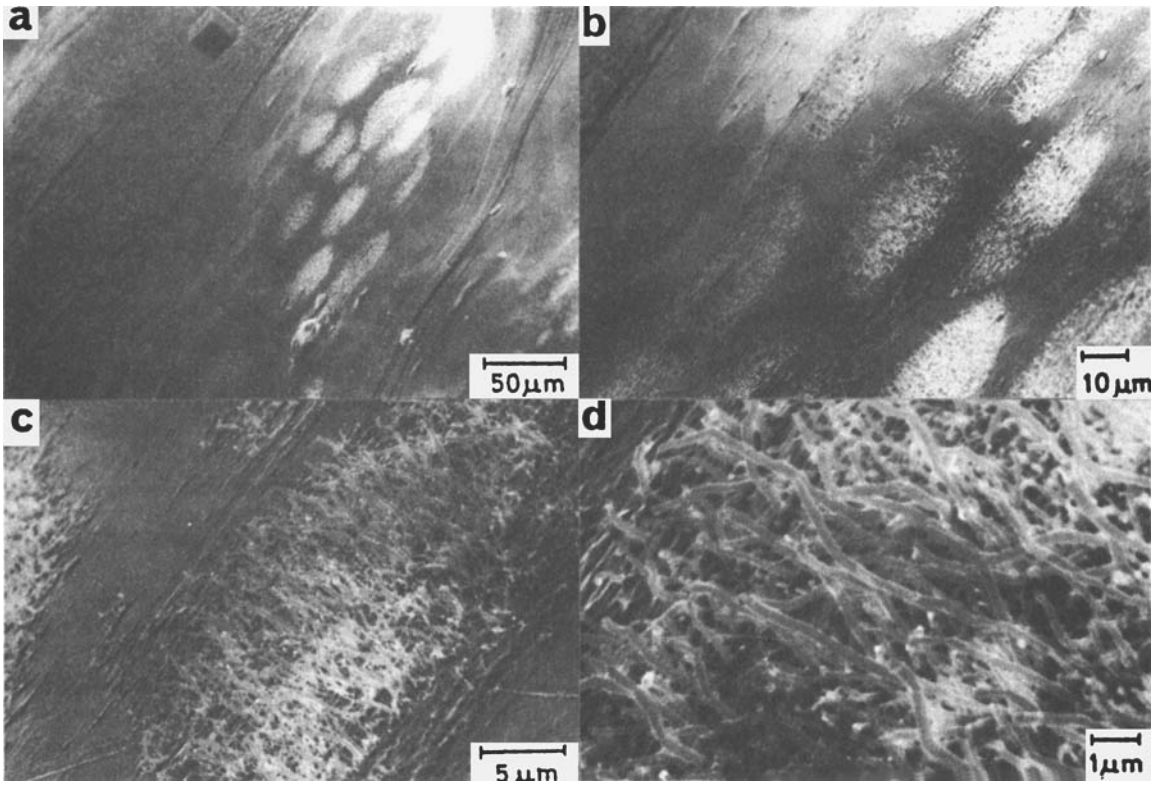

Figure 14. Lateral surface of a PS with 5% pentane sample extruded at 180°C into 60 kPa pressure.
The micrographs show hairlike fibers in circular areas corresponding to previously collapsed miniblisters.

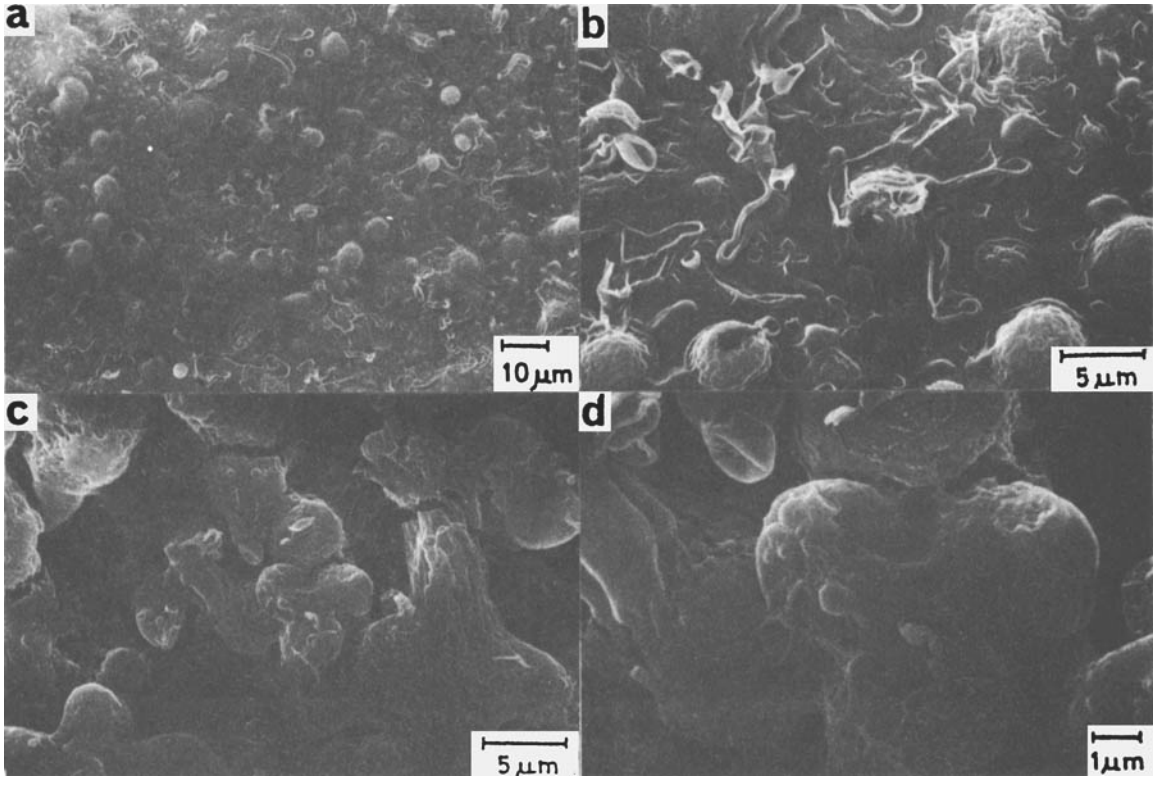

Figure 15. Cross section of PS extruded sample at 170°C into 100 Pa pressure.
a, b. Crusty nodules and collapsed microblisters
c, d. Coalescing nodules forming a larger structure

well as moisture in the system, which in fact may have a positive role in devolatilization. Therefore, completely removing entrained air and adsorbed moisture in the experimental setup—a difficult but possible step—may lead to a system that may misrepresent some of the real systems we are trying to investigate.

Blisters

One of the most striking morphological features discovered in this study is the formation of blisters on the inner surface of the macrobubbles located both on the lateral surface of the strand and in the core of the strand. Figure 8 shows micrographs of the lateral surface of a PS sample extruded at 200°C into 200 Pa pressure. The consecutive enlargements focus on the inner surface of the large macrobubble, clearly revealing rich clusters of blisters. These are thin, dome-shaped, vapor-filled pockets attached to the soft inner surface of the macrobubble. Figure 9 shows the inner surface of a macrobubble within the core of the strand. There are two distinctly different types of blisters: microblisters ranging in size from 1 to 3 μm dia., and miniblisters ranging in size from 10 to 15 μm dia. Figure 9 shows microblisters and miniblisters side by side. This appears to be no coincidence, because it is hypothesized that they evolve from each other. It is suggested that a first generation of microblisters emerges through the soft molten surface of a macrobubble after having been formed as tiny microbubbles under the surface. These styrene-vapor-filled microblisters grow to a maximum diameter of about 3 μm, at which stage the skin containing the vapor is too thin and therefore too weak to withstand the pressure difference, and it bursts releasing the contained vapor into the macrobubble. This behavior is that of microblisters that break through the surface at relatively large (>8 μm) distances from each other. Microblisters emerging closer to each other may merge to form a larger blister with a slightly thicker skin than that of the original blisters. In this manner adjacent microblisters may combine to form a miniblister, as can be seen very clearly in Figure 9. At some stage the miniblister also bursts and the nearly empty skin collapses, entrapping small vapor-filled pockets. These pockets may very well be the nuclei for a second generation of microblisters that grow on the remains of the collapsed miniblister, as can be seen clearly in Figure 10 as well as in Figure 8d. The morphology remaining in a blister-inhabited area at the end of the devolatilization process can be observed in Figure 11. This series of micrographs shows two different types of tracks left by the micro- and miniblisters. The larger tracks (those of the miniblisters) consist of a well-defined circular area in which the surface is rough due to the multilevel remains of the miniblister skin, while the smaller circles are much shallower, revealing the previous presence of single microblisters now gone. Not all macrobubbles are filled with blisters. It is reasonable to assume that when the polymer is depleted of volatiles, no more blisters will form and surface tension heals the inner surface of the macrobubble to a smooth finish.

Blisters are not unique to the PS-styrene system. The remains of miniblisters are clearly seen in Figure 12, which shows micro-

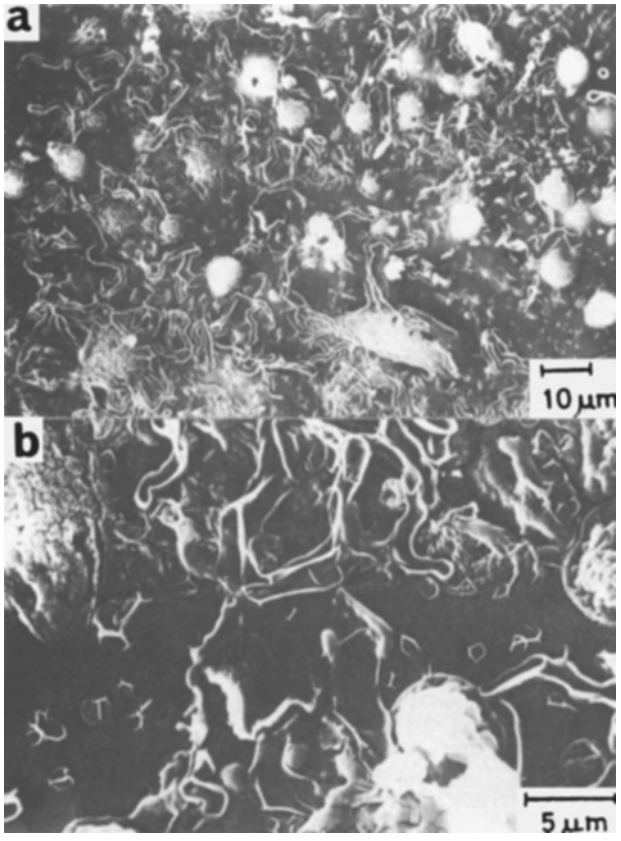

Figure 16. Cross section of a PS extruded sample at 170°C into 100 Pa pressure.
The collapsed crusty nodules convert into a stringy fiberlike structure.

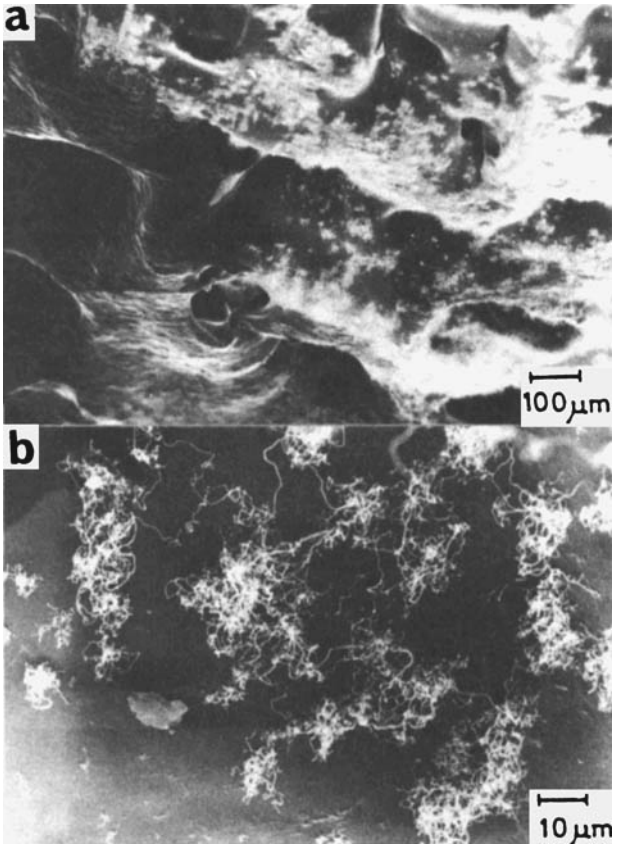

Figure 17. Lateral surface of PS with 5% pentane sample extruded at 170°C into 100 Pa pressure.

graphs of the lateral surface of a PS sample with 5% pentane extruded at 170°C into 100 Pa pressure.

It is important to note that with the PS-styrene system, blisters were more frequently observed at the high end of the temperature range.

Fibrous hair

The micrographs in Figures 13 and 14 show that blisters, in particular miniblisters, may undergo a fascinating transformation into fine hairlike fibers before they fade away into the soft surface of the macrobubble (as in Figure 11). In Figure 13 the formation of short hairlike fibers from a miniblister is clearly seen. The fibers are 0.2–0.3 μm dia. and about 3–5 μm long. Their formation was observed at high temperatures. Hairlike fibers were also observed with the pentane samples, as shown in Figure 14. This figure shows a strand extruded into a relatively high pressure of 60 kPa. The reason for experimenting at such high pressure with the pentane system is that at low pressure levels the superheat is excessive, and some of the fine morphological features may disappear almost instantly.

It is reasonable to assume that in the course of normal devolatilization, that is, without freezing the samples, blisters convert into hairlike structures that in turn collapse into a coarse surface, as shown in Figure 11, and finally, given enough time (of the order of seconds or less) the surfaces become smooth and featureless.

Crusty nodules

At lower extrusion temperatures a crusty nodulelike structure appears; such structures are shown in Figure 15, which is of a thick-skinned blister. Because of the thicker skins, the micro-crusty nodules collapse not like a burst balloon leaving a thin skin, but rather like a deflated football, leaving a pyramid-shaped structure. Thicker skin is also the reason why some mini-crusty nodules tend not to collapse after bursting, but rather release the entrapped vapor through a single craterlike outlet, and then remain as a hollow shell as shown in Figure 15. As a result of the thicker skin and high melt viscosity, micro-crusty nodules appear to merge into larger nodules very slowly, and even adjacent nodules retain their individual shapes, as can be seen very clearly in Figures 15c and 15d.

Stringy fibers

The micrographs shown in Figure 16 show the gradual conversion of crusty nodules into stringy fibers upon the collapse of the nodules and the release of their content. The stringy structure is more clearly seen in the pentane samples shown in Figure 17. They are similar to the foregoing hairlike fibrous structure, but seem to appear at lower temperatures.

Spongy surface

Spongy areas consist of holes of the same order of magnitude as the microblisters. Figure 18 shows the cross section of strands of PS extruded at 170°C into 100 Pa pressure. In spite of the low frequency at which spongy surfaces were encountered, they may be typical microbubbles which in the neighborhood of macrobubbles become blisters or crusty nodules. It is not clear why their frequency of occurrence was so low. They were observed in only two micrographs out of several hundred micrographs taken.

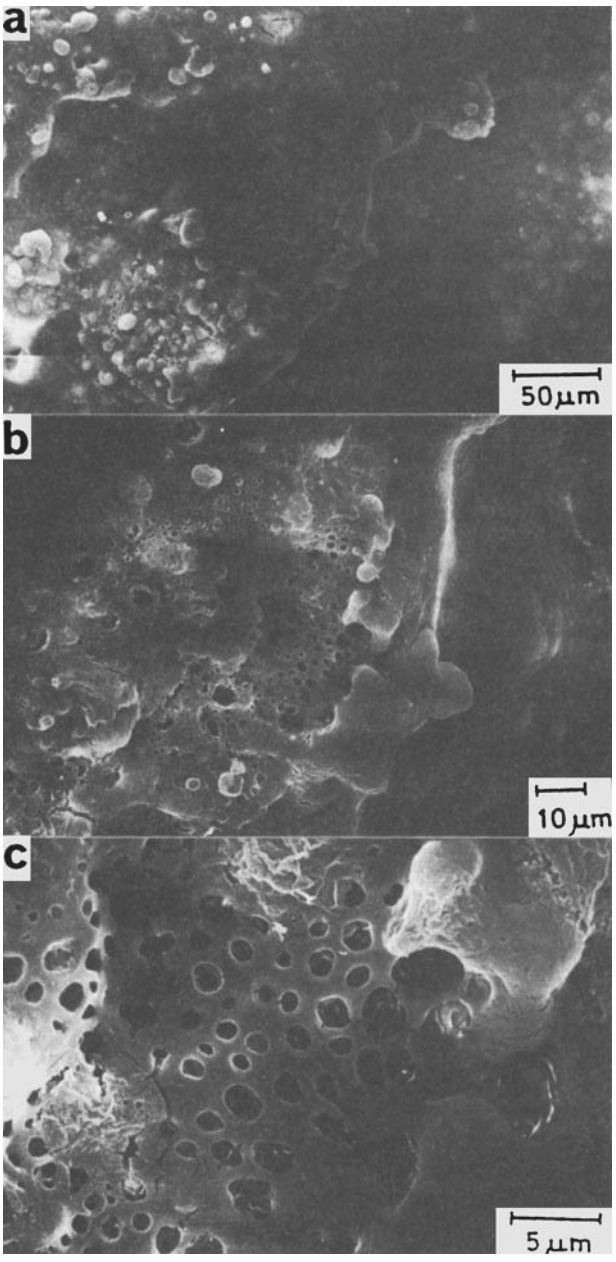

Figure 18. PS sample extruded at 170°C into 90 Pa pressure.
Spongy areas as well as crusty nodules are visible.

Conclusions

In this study a rich variety of morphological features was discovered in polystyrene strands containing styrene and pentane extruded into vacuum. The significance of these morphological features to the devolatilizations process is yet to be established. It is suggested that much of the removal of volatiles at high temperature takes place via a quick sequence of events involving repeated blister growth, rupture, and renucleation. The ruptured blisters release their content into the macrobubbles, and upon the depletion of volatiles the blisters disappear and surface tension quickly heals any remaining signs of the blisters or their byproducts, such as hairlike fibers. A similar process may take

place at lower temperature within the crusty nodules that grow, coalesce, and rupture.

Yet it is possible that the morphological features that were discovered are not inherent to the polymer-solvent system, but are partially due to entrained free air or adsorbed moisture. Therefore, devolatilization of systems free of noncondensable gas and adsorbed moisture and those containing entrained gas or adsorbed moisture may follow different mechanistic routes. Of course, real systems may contain these components; for example, free air may be entrained in the melting steps as well as in rolling pools upstream of the devolatilization zone in screw-extruder and corotating-disk devolatilizers. Moreover, sometimes water or free gas is injected into the molten polymer to enhance the devolatilization process. Therefore, even if free entrained air (or gas) and moisture are not responsible for the observed morphological features, they will certainly affect the devolatilization process directly by increasing the interfacial surface area. Yet, the fact that all the morphological features also appeared with the PS-pentane system seems to indicate that the observations are inherent to the molten polymer-volatile system, rather than being the byproduct of entrained free air or adsorbed moisture. In either case, any serious attempt to quantitatively formulate the devolatilization process must take into account the fact that the process may be far more complex than simple spherical bubble growth in infinite or even finite medium. Moreover, based on the results observed so far it is reasonable to assume that some or all of the features observed in this study may also play a role in rotary equipment characterized by rolling pools and thin films, although the shear fields in the rolling pool may have a profound but yet unknown effect on the whole process.

From a broader physical point of view, the process investigated can be viewed as a study of boiling of a very concentrated viscoelastic solution at low absolute pressures. The relevance of the findings of this study to this problem, however, hinges on the role of free entrained air and adsorbed moisture on the process. The results seem to indicate that the morphological features are inherent to the polymer solution, and therefore the results are relevant to the boiling of such systems. Nevertheless, much additional work is needed to elucidate the full scope and details of such a boiling mechanism.

Acknowledgment

This research was supported by a grant from the National Council for Research and Development, Israel, and the KFA Juelich, Germany. The authors wish to thank the respective institutions for the grant. In addition the authors wish to acknowledge the help of M. Goren, and the Israeli Petrochemical Enterprises for providing polystyrene samples, and O. Zilber for styrene concentration measurements. Finally, the authors wish to thank H. G. Fritz from the Institut fur Kunststofftechnologie at the University of Stuttgart, for discussions and productive cooperation in this project.

Literature cited

Biesenberger, J. A., and D. H. Sebastian, *Principles of Polymerization Engineering*, Wiley-Interscience, New York (1983).

Denson, C. D., "Stripping Operations in Polymer Processing," *Advances in Chemical Engineering*, J. Wei, ed., Academic Press, **12**, 61 (1985).

Hammit, F. G., *Cavitation and Multiphase Flow Phenomena*, McGraw-Hill, New York (1980).

Harvey, E. N., D. K. Barnes, W. D. McElroy, A. H. Whiteley, D. C. Pease, and K. W. Cooper, "Bubble Formation in Animals. I: Physical Factors," *J. Cellular Comp. Physiol.*, **24**(1), 1 (1944a).

Harvey, E. N., A. H. Whiteley, W. D. McElroy, D. C. Pease, and D. K. Barnes, "Bubble Formation in Animals. II: Gas Nuclei and Their Distribution in Blood and Tissues," *J. Cellular Comp. Physiol.*, **24**(1), 23 (1944b).

Newman, R. E., and R. H. M. Simon, "A Mathematical Model of Devolatilization Promoted by Bubble Formation," AIChE 73rd Ann. Meet., Chicago (1980).

Manuscript received June 16, 1986, and revision received Nov. 7, 1986.